Water Research 88 (2016) 127–134

Contents lists available at ScienceDirect

Water Research

journal homepage: www.elsevier.com/locate/watres

$KMnO_4$–Fe(II) pretreatment to enhance *Microcystis aeruginosa* removal by aluminum coagulation: Does it work after long distance transportation?

Jing Qi [a, b], Huachun Lan [a], Shiyu Miao [a], Qiang Xu [a], Ruiping Liu [a], Huijuan Liu [a, *], Jiuhui Qu [a]

[a] Key Laboratory of Drinking Water Science and Technology, Research Center for Eco-Environmental Sciences, Chinese Academy of Sciences, Beijing 100085, China
[b] Graduate School of Chinese Academy of Sciences, Beijing 100039, China

ARTICLE INFO

Article history:
Received 3 July 2015
Received in revised form
27 September 2015
Accepted 2 October 2015
Available online 9 October 2015

Keywords:
Microcystis aeruginosa
Al coagulation
$KMnO_4$–Fe(II) pretreatment
Cell integrity
Settleability evaluation

ABSTRACT

$KMnO_4$–Fe(II) pretreatment was proposed to enhance *Microcystis aeruginosa* (*M. aeruginosa*) removal by aluminum (Al) coagulation in drinking water treatment plants (DWTPs) in our previous study. This study aims to optimize this process and evaluate the feasibility of using the process at water sources, which are usually far away from DWTPs. The optimum molar ratio of $KMnO_4$ to Fe(II) [$R_{KMnO_4:Fe(II)}$] is observed to be 1:3 with respect to algae removal and residual manganese (Mn) control. As indicated from flow cytometer analysis, $KMnO_4$ at <20 μM promisingly maintains cell integrity, with damaged cell ratios of below 10%. $KMnO_4$ at 30 and 60 μM damages *M. aeruginosa* cells more significantly and the damaged cell ratios increase to 21% and 34% after 480 min. The intracellular organic matter (IOM) release can be controlled by the subsequent introduction of Fe(II) to quench residual $KMnO_4$. $KMnO_4$–Fe(II) pretreatment at the $KMnO_4$ dose of 10 μM dramatically enhances the algae removal by over 70% compared to that by Al coagulation, even if $KMnO_4$ and Fe(II) are introduced 480 min prior to the addition of $Al_2(SO_4)_3$. The Al doses can be reduced by more than half to achieve the same algae removal. Furthermore, the deposition of the tiny Fe–Mn precipitates formed rarely occurs, as indicated by a settleability evaluation prior to Al addition. The $KMnO_4$–Fe(II) process can be sequentially dosed at intake points in water sources to achieve moderate inactivation of algae cells and to enhance algae removal in DWTPs thereafter.

1. Introduction

The worldwide occurrence of algae blooms in source water arouses great concern for algae-related water quality globally. Water quality deterioration sometimes occurs due to the penetration of algae cells and the release of odor and taste substances and toxins (Westerhoff et al., 2005; Wert et al., 2014). The algal organic matter (AOM) also serves as precursors to promote formation of disinfection by-products (DBPs) during disinfection (Huang et al., 2009; Fang et al., 2010; Lui et al., 2011; Wei et al., 2011; Zhou et al., 2014a). Additionally, in cases of algae bloom, significantly inhibited treatment is observed due to factors such as poor coagulation and sedimentation efficiency and a significantly shortened filtration cycle (Henderson et al., 2008, 2010; Takaara et al., 2010; Sano et al., 2011; Qu et al., 2012).

Unfortunately, the traditional Al coagulation treatment can hardly achieve satisfactory removal of algae cells due to their negative surface charge, high motility, diverse morphology, and low specific density (Pieterse and Cloot, 1997; Ma et al., 2007; Takaara et al., 2010). It is practically valuable to enhance algae removal on the basis of the conventional treatment processes. Many strategies have been proposed to achieve this goal. Innovations from sedimentation to dissolved air flotation and ultrafiltration processes have been found effective to remove algae cells, with efficiency as high as 90% (Henderson et al., 2008; Yang and Chen, 2013). In addition, electro-coagulation-flotation and hydrodynamic cavitation processes are also attractive (Gao et al., 2010; Li et al., 2014). However, their application is also hindered by the extremely high

* Corresponding author.
E-mail address: hjliu@rcees.ac.cn (H. Liu).

http://dx.doi.org/10.1016/j.watres.2015.10.004
0043-1354/

capital investment required.

The introduction of chemical oxidants, i.e., $KMnO_4$, Cl_2, and O_3, prior to coagulation can also improve algae removal, and the inactivation of algae cells plays a determining role (Ma and Liu, 2002; Chen and Yeh, 2005; Chen et al., 2008, 2009; Shen et al., 2011; Wang et al., 2013). However, excessive inactivation with over-dosed oxidants results in significant rupture of algae cells and the release of IOM accordingly. This effect not only inhibits coagulation and filtration but also increases DBPs formation (Garzon-Sanabria et al., 2013; Feng et al., 2014). To avoid these adverse effects, we have proposed a novel $KMnO_4$–Fe(II) process to achieve a balance between IOM release control and enhanced algae removal (Ma et al., 2012, 2014). The $KMnO_4$–Fe(II) process achieves moderate inactivation of *M. aeruginosa* cells by sequential introduction of $KMnO_4$ and Fe(II). The subsequent-dosed Fe(II) not only halts $KMnO_4$ oxidation but also transforms to *in-situ* Fe(III), with higher coagulation efficiency than preformed Fe(III). In this study, $R_{KMnO_4:Fe(II)}$ was controlled at 1:3, and this should be optimized to achieve its wide-application and to better understand the mechanisms involved. Additionally, the $KMnO_4$–Fe(II) process can also act as a pretreatment prior to Al coagulation, i.e., introduction of $KMnO_4$–Fe(II) 20 min prior to Al salt, to enhance algae removal, involving the dual-coagulant mechanism (Ma et al., 2014).

However, most water sources with algae-related issues, i.e., lakes and reservoirs, are far from the drinking water treatment plants, and it takes several to dozens of hours for the long distance transportation of raw water. Algae at high concentrations are reported to accelerate concrete corrosion and damage pipeline integrity (Setareh and Javaherdashti, 2006; Jayakumar and Saravanane, 2010; Wei et al., 2013). This corrosive effect is caused either by forming tubercles and by generating organic acids, or by developing electrochemical cells (Setareh and Javaherdashti, 2006). The formation of tiny algae flocs prior to or in the water-transporting system is of crucial importance to influence pipeline corrosion. To evaluate the feasibility of applying this $KMnO_4$–Fe(II) process in a long distance transportation system, the following should be well studied: 1) the efficacy of $KMnO_4$ at inactivating algae cells; 2) the efficiency of the $KMnO_4$–Fe(II) process to enhance Al coagulation after long distance transportation; and 3) the probability of the formed tiny flocs settling in the pipeline system.

On the basis of these considerations, this study aims to: 1) optimize the $KMnO_4$–Fe(II) process, i.e., $R_{KMnO_4:Fe(II)}$, $KMnO_4$ dose, and residual Fe/Mn concentration, to improve the algae removal by Al coagulation; 2) evaluate the feasibility of applying this process as a pretreatment in source water.

2. Materials and methods

2.1. Materials and reagents

The algae species used in this study was *M. aeruginosa* because of its prevalence in algae blooms and relevance to water quality and treatment challenges in waterworks (Kemp and John, 2006; Sano et al., 2011). *M. aeruginosa* (strain FACHB-905), previously described by Shen et al. (Shen and Song, 2007), was obtained from Wuhan Institute of Hydrobiology, Chinese Academy of Sciences, and cultured in BG-11 medium (Rippka et al., 1979). The detailed algae growth conditions are presented in Supporting Information (SI). Humic acid was purchased from Sigma–Aldrich (Shanghai) Trading Co., Ltd. SYTOX green nucleic acid stain was purchased from Invitrogen, USA. Other chemical reagents used in the experiments were of analytical grade and solutions were prepared with Milli-Q water. Potassium permanganate ($KMnO_4$) and sodium thiosulfate ($Na_2S_2O_3$) stock solutions of 0.5 g/L were prepared every week and stored in darkness. Ferrous sulfate ($FeSO_4 \cdot 7H_2O$) and aluminum sulfate ($Al_2(SO_4)_3 \cdot 18H_2O$) solutions were prepared just before experiments. Freshly-formed MnO_2 was prepared by mixing $KMnO_4$ and $MnCl_2$ at a molar ratio of 2:3, immediately before being dosed to the algae suspension. Source water was collected from the Qingcaosha reservoir located in Shanghai, China. The basic qualities of source water were as follows: turbidity 3.9–4.2 NTU, pH 7.5–7.7, DOC 3.06–3.52 mg/L. The cultured algae cell density in source water was in the range of 4.2×10^5–4.8×10^5 cells/mL. *M. aeruginosa* was observed to be the dominant algae species (Fig. S1).

2.2. $KMnO_4$–Fe(II) process optimization jar tests

M. aeruginosa cultures were harvested at the exponential growth phase and then diluted with source water to obtain the cell density of 1.0×10^6 cells/mL for all experiments. The pH of this algae suspension was about 7.9. All jar tests were performed with 300 mL samples in 500 mL beakers and conducted on a programmable jar tester (MY3000-6, MeiYu, China). All samples were rapidly mixed at 250 rpm for 5 min after the addition of $KMnO_4$, and Fe(II) was added after the pre-oxidation. The subsequent process consisted of mixing at 200 rpm for 2 min and 40 rpm for 15 min, consecutively. Then, samples were quiescently settled for 30 min.

After settling, samples were siphoned 2 cm below the water surface and divided into two subsamples: the first sample was measured for residual algae by optical density at 680 nm (OD_{680}) with a U-3100 spectrophotometer (Hitachi Co., Japan). The path length of the quartz cell was 10 mm. Milli-Q water served as the control. For each sample, the average OD_{680} value was determined from three measurements. The remaining sample was subjected to filtration through a filter (0.45 μm, glass fiber) and then analyzed for concentrations of Mn and Fe. An inductively coupled plasma optical emission spectrometer (710, Agilent, USA) and/or an inductively coupled plasma mass spectrometer (5000a, Agilent, USA) were used to determine the concentrations of Mn and Fe.

For testing the effects of $R_{KMnO_4:Fe(II)}$, the dose of Fe(II) was fixed at 72 or 90 μM, and $KMnO_4$ (15, 18, 22.5, 30, 45, 90 μM) or (12, 14.4, 18, 24, 36, 72 μM) was added according to $R_{KMnO_4:Fe(II)}$ of 1:6, 1:5, 1:4, 1:3, 1:2, and 1:1. For testing the changes of residual concentrations of Fe and Mn during the whole $KMnO_4$–Fe(II) pretreatment process when $R_{KMnO_4:Fe(II)}$ was fixed at 1:6, the dose of Fe(II) was fixed at 72 or 90 μM. At each predetermined time interval, a sample was withdrawn 2 cm below the water surface and immediately filtered through a 0.45 μm glass fiber filter. The filtered sample was instantly determined for residual Fe(II) by the orthophenanthroline photometric method (Weiss, 1935) and residual Mn by the previously mentioned method. For testing the effects of $KMnO_4$–Fe(II) dose at fixed molar ratio, the doses of $KMnO_4$ were in the range of 15–30 μM, and a threefold molar quantity of Fe(II) was added after the pre-oxidation.

2.3. Cell integrity detection

In order to study the effect of $KMnO_4$ doses on the damage of cell integrity, algae suspensions were rapidly mixed at 250 rpm for 5 min after the addition of $KMnO_4$ (0–60 μM) or MnO_2 (120 μM), and $Na_2S_2O_3$ substituted for Fe(II) was added to quench the oxidation, mixing at 40 rpm for 480 min. Cell integrity was determined for individual cells using a flow cytometer (FACSCalibur 4CLR, BD Biosciences, San Jose, USA) equipped with an argon ion laser emitting at a fixed wavelength of 488 nm for fluorescence measurement. Full details of the cell integrity analysis are presented in Text S2.

2.4. Coagulation method for simulating waterworks treatment process

To investigate the effects of $KMnO_4$–Fe(II) pretreatment on the algae removal by $Al_2(SO_4)_3$ coagulation, samples were mixed at 250 rpm for 5 min soon after dosing with $KMnO_4$ solutions (0–20 μM). Next, Fe(II) solutions at the $R_{KMnO_4:Fe(II)}$ values of 1:3, i.e., 0–60 μM, were added with mixing at 200 rpm for 2 min and then at 40 rpm for 0–480 min to simulate long term transportation. Finally, $Al_2(SO_4)_3$ solution at 20 μM was added, and the samples were then mixed at 200 rpm for 2 min and 40 rpm for 15 min, and the samples were then quiescently settled for 30 min. The supernatants were carefully sampled 2-cm beneath the water surface and the algae concentrations were analyzed accordingly.

The floc growth, i.e., the variation of floc size involved in the abovementioned experiments, was measured with a laser particle size analyzer (Mastersizer 2000, Malvern, UK). The light source comes from a monochromatic coherent He–Ne laser with a fixed wavelength of 633 nm. During the laser diffraction measurement, particles pass through a focused laser beam, and the particles scattering light at an angle is inversely proportional to their size. The angular intensity of the scattered light is then measured by a series of photosensitive detectors. The algae suspension was drawn from the jar through a latex tube to the sample cell of the laser particle size analyzer; and then was returned back to the jar by a peristaltic pump (BT00-300M, Longer, China). To minimize breakage of flocs before measurement, the pump was located downstream of the laser particle size analyzer and was operated at a rate as low as 30 mL/min. The floc median diameter (d_{50}) served as the representative floc size.

2.5. Settling velocity tests

The floc settling velocity after the $KMnO_4$–Fe(II) pretreatment process was tested using a settling column ($D \times H = 100 \times 1000$ mm). After a certain period of settling time, a fixed volume of 500 mL suspension sample was taken from the bottom outlet ($h = 200$ mm). The weight of each sample was measured after being dried. The sediment height data were all recorded before and after taking samples. The details of floc settling velocity calibration are presented in Table S8.

3. Results and discussion

3.1. The optimization of $KMnO_4$–Fe(II) process in M. aeruginosa removal

Fig. 1 illustrates the effects of $R_{KMnO_4:Fe(II)}$ on algae removal and residual Mn concentrations; the Fe(II) doses were 72 and 90 μM, respectively. It can be observed that $KMnO_4$–Fe(II) process at $R_{KMnO_4:Fe(II)}$ of 1:3 resulted in the highest algae removal and lowest residual Mn concentrations. Algae removal increased from 0% to more than 44% with elevated $R_{KMnO_4:Fe(II)}$ from 1:6 to 1:3 (Fig. 1a). The further elevation of $R_{KMnO_4:Fe(II)}$ from 1:3 to 1:1 barely improved algae removal, and the removal efficiency stabilized around 45%.

After sequential introduction of $KMnO_4$ and Fe(II), the reactions involved are complicated. Prior to Fe(II) addition, $KMnO_4$ can react with the organic matter, such as the dissolved organics and the surface-absorbed AOM on algae cells (Eq. (1)) (Xie et al., 2013). The surface-absorbed AOM serves as a protective barrier to stabilize the algae cells, and this effect enhances the difficulty of removing algae cells by conventional processes (Clasen et al., 2000). The oxidation of surface-absorbed AOM benefits the algae removal by destroying the protective barrier of algae cells (Xie et al., 2013), and elevated

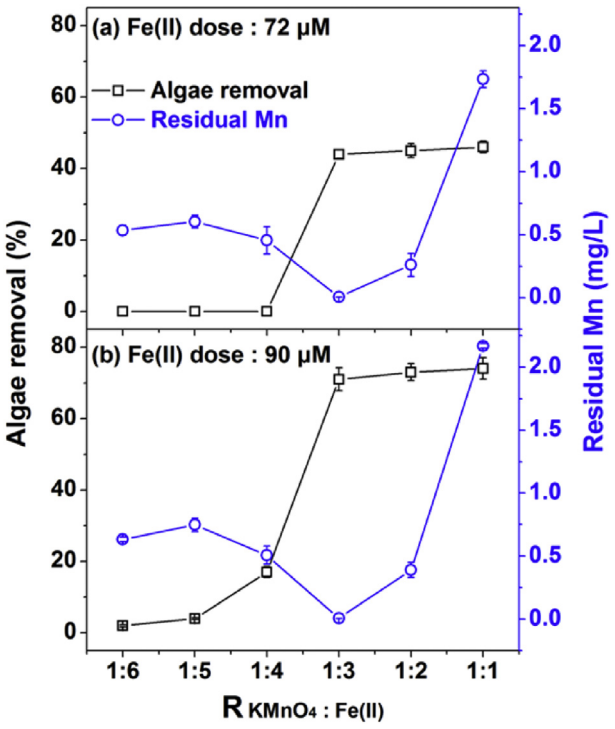

Fig. 1. Effects of $R_{KMnO_4:Fe(II)}$ on algae removal and residual Mn concentrations at Fe(II) doses of (a) 72 μM and (b) 90 μM. Cell density: 1.0×10^6 cells/mL. Mixing procedure: First, $KMnO_4$ was added and mixed by 250 rpm for 5 min; After that, Fe(II) was dosed, mixed by 200 rpm, 2 min and then 40 rpm, 15 min. The results shown are mean data and error bars indicate standard deviations from triplicate analyses.

$KMnO_4$ doses lead to a more significant destruction effect. After the introduction of Fe(II) in $R_{KMnO_4:Fe(II)}$ ranges from 1:6 to 1:3, the residual $KMnO_4$ tends to react with Fe(II) (Eq. (2)) and Fe(II) transforms to *in-situ* formed Fe(III). $KMnO_4$ at elevated doses accelerates the formation of *in-situ* Fe(III) and its content also increases accordingly. The *in-situ* Fe(III) was reported to be more effective than the pre-formed Fe(III) with respect to algae removal, owing to its plentiful reactive surface area and the good efficiency for floc growth (Ma et al., 2012). Fe(II) acts as the source of the *in-situ* Fe(III) and continuously provides it to improve algae removal accordingly. On the other hand, the reduction of $KMnO_4$ by AOM and Fe(II) contributes to its transformation to *in-situ* formed MnO_2. The *in-situ* MnO_2 may act as nuclei to enhance heterogeneous coagulation (Sun et al., 2009). This effect can improve floc growth and sedimentation (Chen and Yeh, 2005), and favor the removal of algae accordingly. At $R_{KMnO_4:Fe(II)}$ of below 1:3, the *in-situ* formed MnO_2 was further reduced to soluble Mn(II) by the subsequently dosed Fe(II) (Eq. (3)), and the removal of algae was relatively low. The formation of *in-situ* MnO_2 was significant at $R_{KMnO_4:Fe(II)}$ of 1:3, as indicated by the lowest residual Mn concentrations at this ratio. Further elevation of $R_{KMnO_4:Fe(II)}$ to 1:1 could hardly increase algae removal, owing to the sufficient amount of $KMnO_4$ to completely oxidize the Fe(II) into *in-situ* Fe(III).

$$MnO_4^- + \text{organic matter} \rightarrow MnO_2 + \text{organic matter}^* \quad (1)$$

$$MnO_4^- + Fe(II) \rightarrow in-situ\ Fe(III) + MnO_2 \quad (2)$$

$$MnO_2 + Fe(II) \rightarrow in-situ\ Fe(III) + Mn^{2+} \quad (3)$$

$$Fe(II) + O_2 \rightarrow in-situ\ Fe(III) \quad (4)$$

The residual Mn concentrations increased with elevated $R_{KMnO_4:Fe(II)}$ from 1:6 to 1:5, due to the complete transformation of $KMnO_4$ to Mn(II) (Eqs. (2) and (3)). However, with $R_{KMnO_4:Fe(II)}$ increasing from 1:5 to 1:3, decreased residual Mn concentrations were observed. At elevated $KMnO_4$ doses, the formation of *in-situ* Fe(III) was favored and the reductive dissolution effect of Fe(II) towards MnO_2 was inhibited, and these combined effects lowered residual Mn levels greatly. Residual Mn showed the minimum concentration of 0.006 mg/L at $R_{KMnO_4:Fe(II)}$ of 1:3, which is far below the Mn maximum contaminant level (MCL) of 0.1 mg/L. At further elevated $R_{KMnO_4:Fe(II)}$ from 1:3 to 1:1, the excessive $KMnO_4$ doses directly increased the residual Mn concentrations, and these results were consistent with the trend obtained by theoretical calculation (Tables S1 and S2). In addition, at the same $KMnO_4$ doses of 24 and 30 μM, the effects of different $R_{KMnO_4:Fe(II)}$, as achieved by varying the Fe(II) doses, on algae removal and residual Mn concentrations were also investigated, and the optimum $R_{KMnO_4:Fe(II)}$ was also observed to be 1:3 (Fig. S2).

To further illustrate the significance of $R_{KMnO_4:Fe(II)}$ on algae removal, the species transformation of Fe and Mn with prolonged contact time was measured at the low $R_{KMnO_4:Fe(II)}$ of 1:6. In the whole slow mixing stage, the residual Mn concentrations varied little and were stable at as high as >0.6 mg/L (Fig. 2a), which corresponded to nearly 73% of the total $KMnO_4$ dose. In this case, the Fe(II) dose was much higher than the stoichiometric amount for reaction with $KMnO_4$, and the excessive Fe(II) completely transformed Mn(IV) oxide into Mn(II) ions (Eqs. (2) and (3)). Additionally, it can be observed in Fig. 2b that the residual Fe(II) concentrations decreased steadily to 0 mg/L even though the $KMnO_4$ dose was insufficient for complete Fe(II) oxidation. This result indicates that dissolved oxygen participated in the oxidization of Fe(II) (Eq. (4)) and played an important role in Fe(II) transformation in case of insufficient $KMnO_4$. The oxidation of Fe(II) by dissolved oxygen has been well studied before and was observed to be improved at elevated pH (Weiss, 1935; Sung and Morgan, 1980). Unfortunately, the algae removal efficiency was as low as 2% (Fig. 1b), although complete transformation of Fe(II) to Fe(III) was achieved. The slight increase of $R_{KMnO_4:Fe(II)}$ from 1:4 to 1:3 resulted in significantly improved algae removal (Fig. 1b), and the *in-situ* formed MnO_2 was inferred to play an important role in algae removal. The *in-situ* formed MnO_2 might play an adsorption role in the aggregation of the tiny flocs and benefit the algae removal process. The element mapping results for the SEM images (Fig. S4) indicate the existence of Fe and Mn in the tiny flocs.

To further optimize the $KMnO_4$–Fe(II) process for algae removal, elevated doses of $KMnO_4$ and Fe(II) were used with the $R_{KMnO_4:Fe(II)}$ controlled at 1:3, and the corresponding algae removal efficiency and the residual concentrations of Fe and Mn are illustrated in Fig. 3. Elevated doses of $KMnO_4$ and Fe(II) contributed to more significant algae removal. $KMnO_4$ at higher doses could contribute to more significant destruction of the protective barrier of algae cells (Clasen et al., 2000; Xie et al., 2013), and the higher amount of the *in-situ* formed MnO_2 also played a positive role. The elevated Fe(II) doses, i.e., the higher *in-situ* Fe(III) concentrations, provided more available coagulant for the destabilization and aggregation of

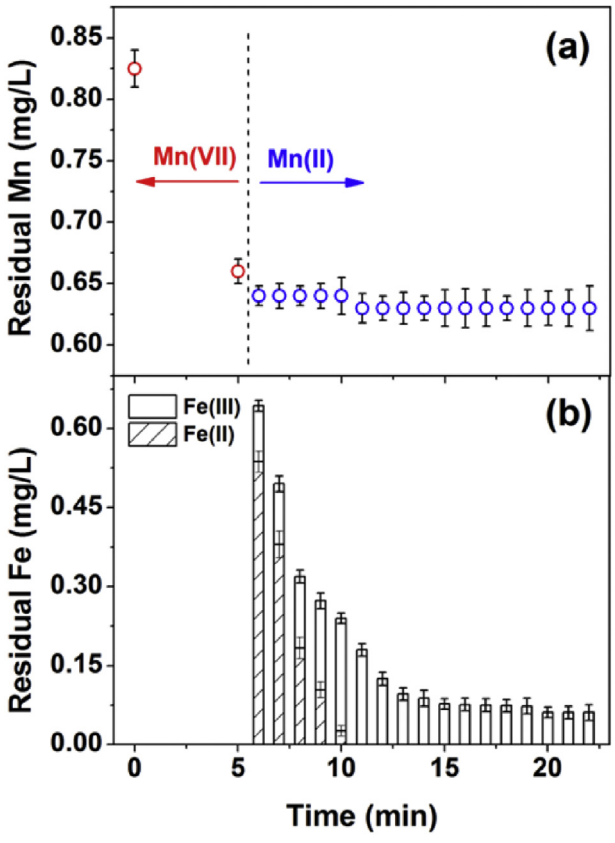

Fig. 2. The variation of (a) residual Mn and (b) residual Fe concentrations during $KMnO_4$–Fe(II) process. $R_{KMnO_4:Fe(II)}$ = 1:6; Fe(II) dose = 90 μM; Cell density: 1.0×10^6 cells/mL. Mixing procedure: First, $KMnO_4$ was added and mixed by 250 rpm for 5 min; After that, Fe(II) was dosed, mixed by 200 rpm, 2 min and then 40 rpm, 15 min. The results shown are mean data and error bars indicate standard deviations from triplicate analyses.

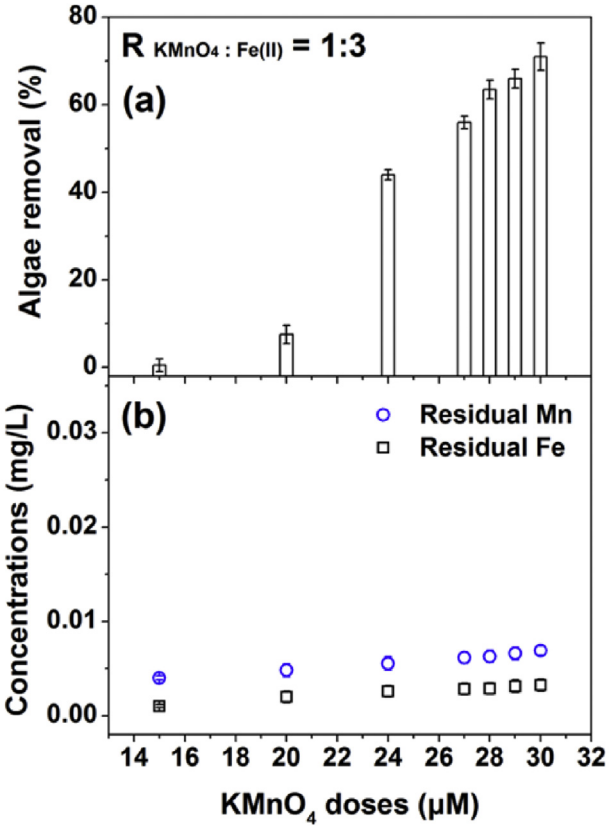

Fig. 3. Effects of $KMnO_4$ doses on (a) algae removal and (b) residual concentrations of Fe and Mn. $R_{KMnO_4:Fe(II)}$ = 1:3; Cell density: 1.0×10^6 cells/mL. Mixing procedure: First, $KMnO_4$ was added and mixed by 250 rpm for 5 min; After that, Fe(II) was dosed, mixed by 200 rpm, 2 min and then 40 rpm, 15 min. The results shown are mean data and error bars indicate standard deviations from triplicate analyses.

algae cells and for floc growth. It was additionally observed that the residual Mn concentrations were consistently below the MCL over a wide $KMnO_4$ dose range from 15 to 30 μM, and Fe(II) at doses stoichiometric for reaction with $KMnO_4$ contributed to the formation of MnO_2, and benefited algae removal accordingly.

These results indicate that the $KMnO_4$–Fe(II) process at $R_{KMnO_4:Fe(II)}$ of 1:3 showed good performance in algae removal and that the residual Mn levels were well controlled at below the MCL. The algae removal efficiency by the $KMnO_4$–Fe(II) process is also observed to be pH-dependent, and elevated pH is beneficial to algae removal (Fig. S5). In case of algae bloom, the source water pH usually increases to the alkaline pH range (Weisz, 1967), and a positive effect may be achieved on $KMnO_4$–Fe(II) pretreatment. However, natural organic matter such as humic acid exhibited an adverse effect on algae removal even at concentrations as low as 1 mg/L as DOC, and elevated doses of $KMnO_4$ and Fe(II) were required to achieve satisfactory algae removal (Fig. S6). Furthermore, there are many different cyanobacterial species in source waters, and they may show significant differences in terms of treatability (Zamyadi et al., 2013), and the feasibility of using this process to enhance their removal should be well evaluated in future studies.

3.2. Effects of $KMnO_4$ doses on *M. aeruginosa* cell integrity

To illustrate the effects of $KMnO_4$ doses on algae cell integrity, $KMnO_4$ at doses from 0 to 60 μM was added and the ratios of damaged algae cells were quantified by flow cytometer (Fig. 4). $KMnO_4$ at doses of below 20 μM showed little effect on algae cells, and the ratios of damaged cells were below 10% after 480 min $KMnO_4$ at 30 μM damaged algae cell integrity greatly, and the ratio of damaged cells was 9.3% after quenching $KMnO_4$ for 60 min, and then increased to 21.2% after 480 min. More significant damage of algae cells, i.e., 34.8%, was observed at 60 μM $KMnO_4$.

$KMnO_4$ at low doses, i.e., below 20 μM, mainly reacted with the surface-absorbed AOM rather than directly damaging algae cells. This result is consistent with the previous findings that algae cells oxidized by lower doses of $KMnO_4$ can still keep their integrity (Chen and Yeh, 2005; Xie et al., 2013; Fan et al., 2014). Oxidants like $KMnO_4$, H_2O_2, $CuSO_4$, ozone and chlorine have all been proved to be capable of damaging algae cells using flow cytometer, but the damage level is highly dependent on the oxidant dose and exposure time (Wert et al., 2013; Fan et al., 2014; Zhou et al., 2014b). Interestingly, the 5-min exposure to $KMnO_4$ also mainly damaged the protective barrier rather than inactivating algae cells, as indicated from the low ratios of damaged cells even at $KMnO_4$ dose of as high as 60 μM. However, the algae cell damage continued with prolonged transportation time and the ratios of damaged cells increased, even though the residual $KMnO_4$ was completely quenched. It should be noted that $Na_2S_2O_3$ was dosed soon after the 5-min rapid mixing period to quench the residual $KMnO_4$ to MnO_2. The freshly prepared *in-situ* MnO_2 is a solid oxidant and is widely used for the oxidation of arylmethylene compounds, pyrene, sulfadiazine and arsenite (Dong et al., 2009; Li et al., 2010; Chien et al., 2011; Nammalwar et al., 2013). However, the *in-situ* MnO_2 showed little oxidative efficacy towards algae cells and caused little damage to algae cells even at doses as high as 120 μM. The damage of algae cells was attributed to the oxidative effect of $KMnO_4$ rather than that of the *in-situ* MnO_2. Chemical oxidants such as H_2O_2 have been reported to induce oxidative stress to algae cells and cause the programmed cell death (PCD) of algae cells (Ross et al., 2006; Ding et al., 2012; Mikula et al., 2012), and this effect can induce the rapid collapse of *M. aeruginosa* bloom (Kaneko et al., 2007; Frangeul et al., 2008). PCD is a genetically controlled form of cell suicide (Ameisen, 2002), which could be induced by heat, nutrient deprivation, salt stress, ultraviolet irradiation, and oxidative stress (Bidle and Falkowski, 2004; Bidle et al., 2007). The membrane disintegration of algae cells by $KMnO_4$ might serve as a signal for PCD, and this effect may account for the increase of damaged cells with prolonged transportation time even after the complete quenching of $KMnO_4$.

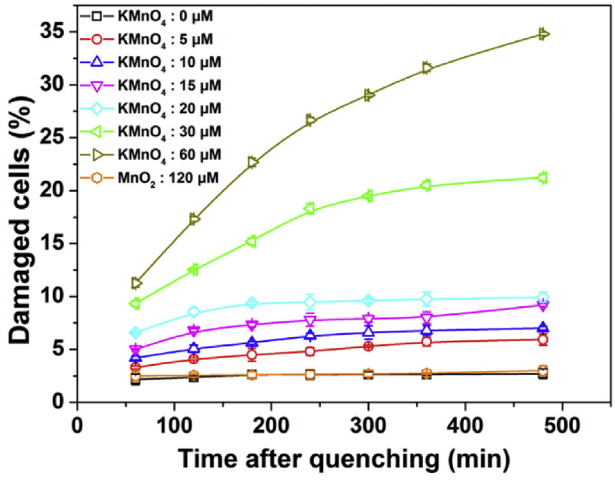

Fig. 4. Effects of $KMnO_4$ doses on the damage of algae cell integrity within simulated transportation time of 480 min. Cell density: 1.0×10^6 cells/mL. Pre-oxidation procedure: 250 rpm, 5 min; $Na_2S_2O_3$ was dosed to quench residual oxidants soon after pre-oxidation. Mixing speed:40 rpm. The results shown are mean data and error bars indicate standard deviations from triplicate analyses.

It has been reported that oxidants such as ozone and chlorine result in algae cell rupture, and the damaged cells tend to release remarkable amounts of IOM and adversely affect waterworks to a large extent (Garzon-Sanabria et al., 2013; Feng et al., 2014). These results indicate that the integrity of algae cells is highly dependent on the $KMnO_4$ dose and the time for water transportation from source water to DWTPs, i.e., the water transportation period. If the water transportation period was lower than 60 min, the algae cell damage and IOM release might be well controlled in a wide $KMnO_4$ dose range from 5 to 60 μM. Otherwise, lower $KMnO_4$ doses of 5–20 μM should be used to avoid significant IOM release in the long term transportation of source water. $KMnO_4$ at 20 μM rarely contributed to IOM release, as indicated from the stable DOC concentrations with prolonged transportation time (Table S5). The commonly used $KMnO_4$ doses are in the range from 0.5 to 3 mg/L (Knappe et al., 2004), and the dose of 20 μM i.e., 3.16 mg/L, is practically enough in engineering point-of-view.

3.3. Effects of $KMnO_4$–Fe(II) pretreatment on *M. aeruginosa* removal by Al coagulation

Fig. 5 indicates that $KMnO_4$–Fe(II) pretreatment can show positive effects on Al coagulation even after long distance transportation of 8 h. $KMnO_4$–Fe(II) pretreatment at $KMnO_4$ doses of 10 and 20 μM dramatically increased algae removal to 72% and 91%, respectively. The time intervals between dosing Fe(II) and $Al_2(SO_4)_3$ may show effects on algae removal; however, the extent is much too low and is negligible. This can be explained by the low ratios of damaged cells found, as shown in Fig. 4, which play an important role in avoiding significant IOM release and coagulation disturbance. Additionally, $KMnO_4$–Fe(II) pretreatment can greatly reduce the required Al doses to achieve the same algae removal efficiency by Al coagulation. Without $KMnO_4$–Fe(II) pretreatment, $Al_2(SO_4)_3$ coagulation resulted in algae removal efficiency of as low as 2%, and $Al_2(SO_4)_3$ dose of 50 μM was required to achieve the algae removal

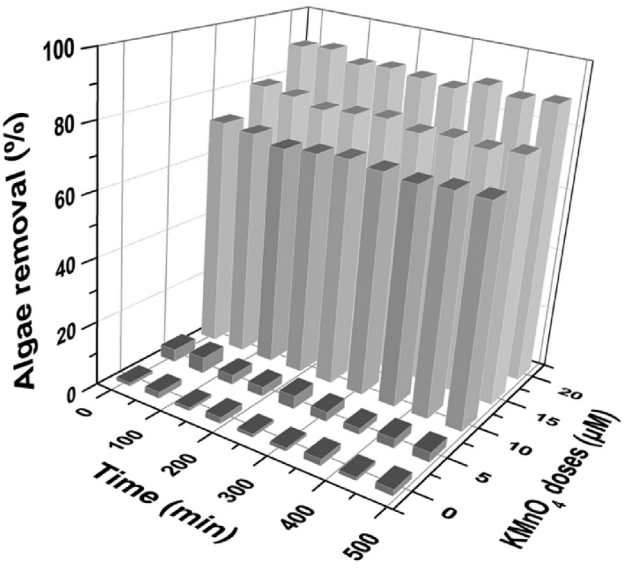

Fig. 5. Effects of $KMnO_4$ doses and time intervals between dosing Fe(II) and $Al_2(SO_4)_3$ on algae removal. Cell density: 1.0×10^6 cells/mL; $R_{KMnO_4:Fe(II)} = 1{:}3$; $Al_2(SO_4)_3$ dose = 20 μM. Mixing procedure: First, $KMnO_4$ (if any) was added and mixed by 250 rpm for 5 min; After that, Fe(II) (if any) was dosed, mixed by 200 rpm, 2 min and then 40 rpm, 0–480 min; Finally, $Al_2(SO_4)_3$ was dosed, mixed by 200 rpm, 2 min and then 40 rpm, 15 min.

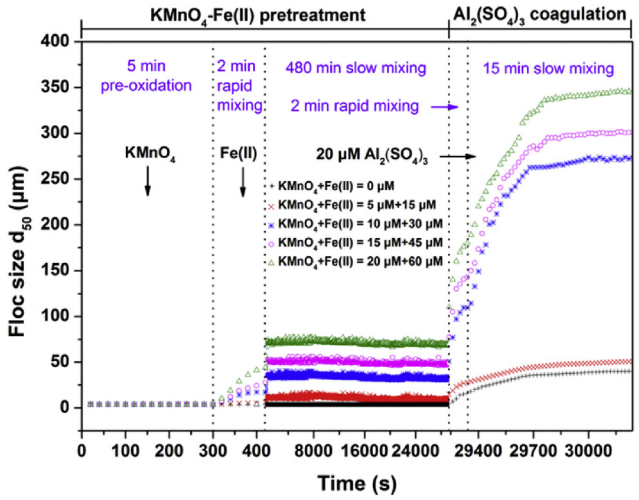

Fig. 6. Effects of $KMnO_4$–Fe(II) pretreatment on floc growth within simulated transportation time of 480 min. Cell density: 1.0×10^6 cells/mL; $R_{KMnO_4:Fe(II)} = 1{:}3$; $Al_2(SO_4)_3$ dose = 20 μM. Mixing procedure: First, $KMnO_4$ (if any) was added and mixed by 250 rpm for 5 min; After that, Fe(II) (if any) was dosed, mixed by 200 rpm, 2 min and then 40 rpm, 480 min; Finally, $Al_2(SO_4)_3$ was dosed, mixed by 200 rpm, 2 min and then 40 rpm, 15 min.

efficiency of 75% (Fig. S7). $KMnO_4$–Fe(II) pretreatment, at $KMnO_4$ dose of as low as 10 μM, decreased the required $Al_2(SO_4)_3$ dose by more than half, to as low as 20 μM. Ma and Liu (2002) reported low algae removal efficiency of near 30% even at the high $Al_2(SO_4)_3$ dose of 50 μM in the Cell density range from 8×10^6 to 2×10^7 cells/L (Ma and Liu, 2002). The tiny flocs formed in the $KMnO_4$–Fe(II) process dominate in the enhanced Al coagulation at the relatively low $Al_2(SO_4)_3$ dose of 20 μM, and the reported synergistic effects between Fe and Al as dual-coagulants (Ma et al., 2014) may also play an important role.

Several treatment plants use Qingcaosha reservoir as a water source, and in case of algae bloom, Cl_2 at 1.0–1.5 mg/L and $Al_2(SO_4)_3$ at 20–50 mg/L were respectively dosed at the intake point and the rapid-mixing unit in the plant. Table S7 compares the reagent costs between the currently-used process and this process, and the $KMnO_4$–Fe(II) pretreatment is observed to be a cost-effective and economically valuable way to enhance algae removal by Al coagulation. Besides the effect on cost, the significantly shortened filtration cycle as observed in case of algae bloom (Qu et al., 2012) may be greatly avoided due to the much higher algae removal prior to the filters.

3.4. Settleability evaluation on the formed flocs in $KMnO_4$–Fe(II) process

From an engineering point-of-view, the settleability of the flocs formed in the $KMnO_4$–Fe(II) process should be well evaluated to avoid their deposition in pipelines. Fig. 6 illustrates the floc size variation within the long simulated transportation time of 480 min. At $KMnO_4$ doses of above 10 μM, the average diameter of the formed tiny flocs was stable at less than 77 μm in the long-term simulated transportation period, and the introduction of $Al_2(SO_4)_3$ remarkably improved particle aggregation and the floc size increased to as high as above 273 μm soon after dosing with $Al_2(SO_4)_3$. These results indicate that the formed flocs in the $KMnO_4$–Fe(II) process were unlikely to deposit in transportation pipelines.

Table 1 illustrates the maximum d_{50} in different treatment processes in a wide range of $KMnO_4$ doses from 0 to 20 μM. In the $KMnO_4$ oxidation period, i.e., the initial 5 min, the maximum d_{50} values were about 4 μm and independent of the $KMnO_4$ doses. The observed d_{50} were indicative of algae cells and were consistent with what had been reported before (Baskan and Pala, 2010). The introduction of Fe(II) and its transformation to *in-situ* Fe(III) contributed to the increased d_{50} values in the 2-min rapid mixing stage, and higher values were observed at elevated doses of $KMnO_4$ and Fe(II). During the 480-min slow mixing stage, i.e., $KMnO_4$ dose of 20 μM, d_{50} values continued to increase from 44 μm to 66 μm at first, and then were stable in the range from 66 to 77 μm. The introduction of Al contributed to floc growth in the rapid and slow mixing stages and finally achieved stable d_{50} values.

To further evaluate the settleability of the flocs in transportation pipes, the non-depositing critical velocity (v_s) as proposed by Nalluri et al. was used (Nalluri et al., 1992, 1994; Nalluri and Spaliviero, 1998). At the maximum $KMnO_4$ dose of 20 μM, the maximum d_{50} value of 77 μm was observed.

The Reynolds number (Re) is calculated by Eq. (5) as follows:

$$\mathrm{Re} = \frac{vD}{\nu} \tag{5}$$

v = pipe flow velocity (assumed, v = 0.6 m/s); D = pipe diameter (assumed, 3 m); ν = Water kinematic viscosity coefficient (293.15 K, $\nu = 1.01 \times 10^{-6}$ m^2/s).

On the basis of Re, the frictional resistance coefficient (λ) and total frictional resistance coefficient (λ_s) can be calculated by Eqs. (6) and (7) as follows:

$$\lambda = 0.0032 + \frac{0.221}{Re^{0.237}} \quad \left(10^5 < Re < 3 \times 10^6\right) \tag{6}$$

$$\lambda_s = 5.3\, C_V{}^{0.0145} \left(\frac{D}{y_0}\right)^{0.0435} \lambda^{1.363} \tag{7}$$

C_V = Floc volume concentration (Text S3, $C_V = 9.3 \times 10^{-5}$); y_0 = water depth (assumed, 1.5 m).

Next, the floc density to water density ratio (S) can be calculated

Table 1
Maximum d_{50} (μm) during the whole treatment process.

$KMnO_4$	Fe(II)	5-min pre-oxidation	2-min rapid mixing	480-min slow mixing	2-min rapid mixing	15-min slow mixing
0	0	4.0	4.0	4.1	16.0	40.0
5	15	4.0	6.1	16.9	28.0	50.9
10	30	4.0	17.4	40.6	109.6	273.8
15	45	4.0	27.9	55.9	142.8	301.4
20	60	4.0	44.0	76.7	180.0	345.7

by Eq. (8):

$$S = \rho_s/\rho \tag{8}$$

ρ = Water density (293.15 K, 101.324 × 10^3 Pa, ρ = 0.998 × 10^3 kg/m^3); ρ_s = Floc density (Text S3, $\rho_s = 1.030 \times 10^3$ kg/m^3).

Finally, v_s can be obtained by Eq. (9) as follows:

$$v_s = 2.56\sqrt{gd(S-1)}C_V{}^{0.165}\left(\frac{y_0}{D}\right)^{0.4}\left(\frac{d}{D}\right)^{-0.57}\lambda_s{}^{0.10} \tag{9}$$

g = gravitational acceleration (9.8 m/s^2); d = median diameter (d_{50}).

According to the above calculation, the non-depositing critical velocity is calculated to be 0.54 m/s, which is lower than the assumed pipe flow velocity (0.6 m/s). The velocity gradient (G) of the assumed water condition is calculated to be 16^{-s} (Text S4) which is the same as the one observed in the programmable jar tester when mixed at 40 rpm. Therefore, the formed flocs during the $KMnO_4$–Fe(II) process are inferred to be unlikely to deposit in the transportation pipes even at the highest $KMnO_4$ dose of 20 μM. In regards to the various flow velocities and pipe diameters in different pipeline systems, the floc size can be controlled by optimizing the doses of $KMnO_4$ and Fe(II) and adapted to different values of non-depositing critical velocity.

4. Conclusions

This study indicates that $KMnO_4$ and Fe(II) can be dosed in sequence at the intake points of source water as pretreatment to enhance algae removal by conventional Al coagulation. The optimum $R_{KMnO_4:Fe(II)}$ is observed to be 1:3 to achieve maximum algae removal and to minimize residual Mn as well. The 5-min exposure to $KMnO_4$ at doses of below 20 μM can hardly damage the integrity of algae cells, and the ratios of damaged cells are below 10%. The release of IOM from damaged algae cells can be well avoided even after 480 min. The formed flocs during the $KMnO_4$–Fe(II) process are unlikely to deposit in the long-term transportation pipelines, and pipeline clogging can be avoided as much as possible. Additionally, $KMnO_4$–Fe(II) pretreatment can reduce the required Al doses by more than half to achieve the same algae removal efficiency. $KMnO_4$–Fe(II) pretreatment achieves high algae removal efficiency, and residual Fe/Mn levels can be well controlled to below their MCLs. In addition, the implementation of $KMnO_4$–Fe(II) pretreatment requires little reconstruction of the existing DWTPs and savings in reagent costs can even be realized to some extent. Implementation of $KMnO_4$–Fe(II) pretreatment may be practically applicable to many DWTPs for enhancing algae removal and controlling IOM release in cases of algae bloom.

Acknowledgments

This work was supported by the National Science Fund for Distinguished Young Scholars of China (Grant No. 51225805) and the National Natural Science Foundation of China (Grant No. 51422813).

Appendix A. Supplementary data

Supplementary data related to this article can be found at http://dx.doi.org/10.1016/j.watres.2015.10.004.

References

Ameisen, J.C., 2002. On the origin, evolution, and nature of programmed cell death: a timeline of four billion years. Cell Death Differ. 9 (4), 367–393.
Baskan, M.B., Pala, A., 2010. A statistical experiment design approach for arsenic removal by coagulation process using aluminum sulfate. Desalination 254 (1–3), 42–48.
Bidle, K.D., Falkowski, P.G., 2004. Cell death in planktonic, photosynthetic microorganisms. Nat. Rev. Microbiol. 2 (8), 643–655.
Bidle, K.D., Haramaty, L., Barcelos e Ramos, J., Falkowski, P., 2007. Viral activation and recruitment of metacaspases in the unicellular coccolithophore, *Emiliania huxleyi*. Proc. Natl. Acad. Sci. U. S. A. 104 (14), 6049–6054.
Chen, J.-J., Yeh, H.-H., 2005. The mechanisms of potassium permanganate on algae removal. Water Res. 39 (18), 4420–4428.
Chen, J.-J., Yeh, H.-H., Tseng, I.-C., 2008. Potassium permanganate as an alternative preoxidant for enhancing algal coagulation – pilot and bench scale studies. Environ. Technol. 29 (7), 721–729.
Chen, J.-J., Yeh, H.-H., Tseng, I.-C., 2009. Effect of ozone and permanganate on algae coagulation removal – pilot and bench scale tests. Chemosphere 74 (6), 840–846.
Chien, S.W.C., Chang, C.H., Chen, S.H., Wang, M.C., Rao, M.M., Veni, S.S., 2011. Oxidative degradation of pyrene in contaminated soils by delta-MnO_2 with or without sunlight irradiation. Sci. Total Environ. 409 (19), 4078–4086.
Clasen, J., Mischke, U., Drikas, M., Chow, C., 2000. An improved method for detecting electrophoretic mobility of algae during the destabilisation process of flocculation: flocculant demand of different species and the impact of DOC. J. Water Serv. Res. Technol.-Aqua 49 (2), 89–101.
Ding, Y., Gan, N.Q., Li, J., Sedmak, B.J., Song, L.R., 2012. Hydrogen peroxide induces apoptotic-like cell death in *Microcystis aeruginosa* (Chroococcales, Cyanobacteria) in a dose-dependent manner. Phycologia 51 (5), 567–575.
Dong, J., Li, Y.T., Zhang, L.J., Liu, C.S., Zhuang, L., Sun, L.N., Zhou, J.M., 2009. The oxidative degradation of sulfadiazine at the interface of alpha-MnO_2 and water. J. Chem. Technol. Biotechnol. 84 (12), 1848–1853.
Fan, J.J., Hobson, P., Ho, L., Daly, R., Brookes, J., 2014. The effects of various control and water treatment processes on the membrane integrity and toxin fate of cyanobacteria. J. Hazard. Mater. 264, 313–322.
Fang, J.Y., Yang, X., Ma, J., Shang, C., Zhao, Q.A., 2010. Characterization of algal organic matter and formation of DBPs from chlor(am)ination. Water Res. 44 (20), 5897–5906.
Feng, G.Z., Chu, H.Q., Dong, B.Z., 2014. Fouling effects of algogenic organic matters during nanofiltration of naproxen. Desalination 350, 69–78.
Frangeul, L., Quillardet, P., Castets, A.-M., Humbert, J.-F., Matthijs, H.C.P., Cortez, D., Tolonen, A., Zhang, C.-C., Gribaldo, S., Kehr, J.-C., Zilliges, Y., Ziemert, N., Becker, S., Talla, E., Latifi, A., Billault, A., Lepelletier, A., Dittmann, E., Bouchier, C., de Marsac, N.T., 2008. Highly plastic genome of *Microcystis aeruginosa* PCC 7806, a ubiquitous toxic freshwater cyanobacterium. Bmc Genomics 9.
Gao, S.S., Du, M.A., Tian, J.Y., Yang, J.Y., Yang, J.X., Ma, F., Nan, J., 2010. Effects of chloride ions on electro-coagulation-flotation process with aluminum electrodes for algae removal. J. Hazard. Mater. 182 (1–3), 827–834.
Garzon-Sanabria, A.J., Ramirez-Caballero, S.S., Moss, F.E.P., Nikolov, Z.L., 2013. Effect of algogenic organic matter (AOM) and sodium chloride on nannochloropsis salina flocculation efficiency. Bioresour. Technol. 143, 231–237.
Henderson, R., Parsons, S.A., Jefferson, B., 2008. The impact of algal properties and pre-oxidation on solid–liquid separation of algae. Water Res. 42 (8–9), 1827–1845.
Henderson, R.K., Parsons, S.A., Jefferson, B., 2010. The impact of differing cell and algogenic organic matter (AOM) characteristics on the coagulation and flotation of algae. Water Res. 44 (12), 3617–3624.
Huang, J., Graham, N., Templeton, M.R., Zhang, Y., Collins, C., Nieuwenhuijsen, M., 2009. A comparison of the role of two blue-green algae in THM and HAA formation. Water Res. 43 (12), 3009–3018.
Jayakumar, S., Saravanane, R., 2010. Biodeterioration of coastal concrete structures

by Marine green algae. Int. J. Civ. Eng. 8 (4), 352–361.
Kaneko, T., Nakajima, N., Okamoto, S., Suzuki, I., Tanabe, Y., Tamaoki, M., Nakamura, Y., Kasai, F., Watanabe, A., Kawashima, K., Kishida, Y., Ono, A., Shimizu, Y., Takahashi, C., Minami, C., Fujishiro, T., Kohara, M., Katoh, M., Nakazaki, N., Nakayama, S., Yamada, M., Tabatai, S., Watanabe, M.M., 2007. Complete genomic structure of the bloom-forming toxic cyanobacterium *Microcystis aeruginosa* NIES-843. DNA Res. 14 (6), 247–256.
Kemp, A., John, J., 2006. Microcystins associated with Microcystis dominated blooms in the southwest wetlands, Western Australia. Environ. Toxicol. 21 (2), 125–130.
Knappe, R., Detlef, R.U., Belk, C., Briley, D.S., Grandy, S.R., Rastogi, N., Rike, A.H., 2004. Algae Detection and Removal Strategies for Drinking Water Treatment Plants. AWWA Research Foundation, Denver, USA.
Li, P., Song, Y., Yu, S.L., 2014. Removal of *Microcystis aeruginosa* using hydrodynamic cavitation: performance and mechanisms. Water Res. 62, 241–248.
Li, X.J., Liu, C.S., Li, F.B., Li, Y.T., Zhang, L.J., Liu, C.P., Zhou, Y.Z., 2010. The oxidative transformation of sodium arsenite at the interface of alpha-MnO_2 and water. J. Hazard. Mater. 173 (1–3), 675–681.
Lui, Y.S., Qiu, J.W., Zhang, Y.L., Wong, M.H., Liang, Y., 2011. Algal-derived organic matter as precursors of disinfection by-products and mutagens upon chlorination. Water Res. 45 (3), 1454–1462.
Ma, J., Lei, G.Y., Fang, J.Y., 2007. Effect of algae species population structure on their removal by coagulation and filtration processes – a case study. J. Water Supply Res. Technol.-Aqua 56 (1), 41–54.
Ma, J., Liu, W., 2002. Effectiveness and mechanism of potassium ferrate(VI) preoxidation for algae removal by coagulation. Water Res. 36 (4), 871–878.
Ma, M., Liu, R.P., Liu, H.J., Qu, J.H., 2012. Effect of moderate pre-oxidation on the removal of *Microcystis aeruginosa* by $KMnO_4$–Fe(II) process: significance of the in-situ formed Fe(III). Water Res. 46 (1), 73–81.
Ma, M., Liu, R.P., Liu, H.J., Qu, J.H., 2014. Mn(VII)–Fe(II) pre-treatment for *Microcystis aeruginosa* removal by Al coagulation: simultaneous enhanced cyanobacterium removal and residual coagulant control. Water Res. 65, 73–84.
Mikula, P., Zezulka, S., Jancula, D., Marsalek, B., 2012. Metabolic activity and membrane integrity changes in *Microcystis aeruginosa* – new findings on hydrogen peroxide toxicity in cyanobacteria. Eur. J. Phycol. 47 (3), 195–206.
Nalluri, C., Alvarez, E.M., Ghani, A.A., Elzaemey, A., 1992. The influence of cohesion on sediment behavior. Water Sci. Technol. 25 (8), 151–164.
Nalluri, C., Ghani, A.A., Elzaemey, A., 1994. Sediment transport over deposited beds in sewers. Water Sci. Technol. 29 (1–2), 125–133.
Nalluri, C., Spaliviero, F., 1998. Suspended sediment transport in rigid boundary channels at limit deposition. Water Sci. Technol. 37 (1), 147–154.
Nammalwar, B., Fortenberry, C., Bunce, R.A., Lageshetty, S.K., Ausman, K.D., 2013. Efficient oxidation of arylmethylene compounds using nano-MnO_2. Tetrahedron Lett. 54 (15), 2010–2013.
Pieterse, A., Cloot, A., 1997. Algal cells and coagulation, flocculation and sedimentation processes. Water Sci. Technol. 36 (4), 111–118.
Qu, F.S., Liang, H., He, J.G., Ma, J., Wang, Z.Z., Yu, H.R., Li, G.B., 2012. Characterization of dissolved extracellular organic matter (dEOM) and bound extracellular organic matter (bEOM) of *Microcystis aeruginosa* and their impacts on UF membrane fouling. Water Res. 46 (9), 2881–2890.
Rippka, R., Deruelles, J., Waterbury, J.B., Herdman, M., Stanier, R.Y., Mar 1979. Generic assignments, strain histories and properties of pure cultures of cyanobacteria. J. Gen. Microbiol. 111, 1–61.
Ross, C., Santiago-Vázquez, L., Paul, V., 2006. Toxin release in response to oxidative stress and programmed cell death in the cyanobacterium *Microcystis aeruginosa*. Aquat. Toxicol. 78 (1), 66–73.
Sano, D., Ishifuji, S., Sato, Y., Imae, Y., Takaara, T., Masago, Y., Omura, T., 2011. Identification and characterization of coagulation inhibitor proteins derived from cyanobacterium *Microcystis aeruginosa*. Chemosphere 82 (8), 1096–1102.
Setareh, M., Javaherdashti, R., 2006. Evaluation of sessile microorganisms in pipelines and cooling towers of some Iranian industries. J. Mater. Eng. Perform. 15 (1), 5–8.
Shen, H., Song, L.R., 2007. Comparative studies on physiological responses to phosphorus in two phenotypes of bloom-forming microcystis. Hydrobiologia 592, 475–486.
Shen, Q.H., Zhu, J.W., Cheng, L.H., Zhang, J.H., Zhang, Z., Xu, X.H., 2011. Enhanced algae removal by drinking water treatment of chlorination coupled with coagulation. Desalination 271 (1–3), 236–240.
Sun, L.H., Liu, R.P., Xia, S.J., Yang, Y.L., Li, G.B., 2009. Enhanced As(III) removal with permanganate oxidation, ferric chloride precipitation and sand filtration as pretreatment of ultrafiltration. Desalination 243 (1–3), 122–131.
Sung, W., Morgan, J.J., 1980. Kinetics and product of ferrous iron oxygenation in aqueous systems. Environ. Sci. Technol. 14 (5), 561–568.
Takaara, T., Sano, D., Masago, Y., Omura, T., 2010. Surface-retained organic matter of *Microcystis aeruginosa* inhibiting coagulation with polyaluminum chloride in drinking water treatment. Water Res. 44 (13), 3781–3786.
Wang, L., Qiao, J.L., Hu, Y.H., Zhang, L., Zhou, Q.L., Gao, N.Y., 2013. Pre-oxidation with $KMnO_4$ changes extra-cellular organic matter's secretion characteristics to improve algal removal by coagulation with a low dosage of polyaluminium chloride. J. Environ. Sci.-China 25 (3), 452–459.
Wei, S.P., Jiang, Z.L., Liu, H., Zhou, D.S., Sanchez-Silva, M., 2013. Microbiologically induced deterioration of concrete – a review. Braz. J. Microbiol. 44 (4), 1001–1007.
Wei, Y.Y., Liu, Y., Dai, R.H., Liu, X., Wu, J.J., Shi, Z., Ren, J., Zhang, Y., 2011. Trihalomethanes and haloacetic acid species from the chlorination of algal organic matter and bromide. Water Sci. Technol. 63 (6), 1111–1120.
Weiss, J., 1935. Elektronenübergangsprozesse im Mechanismus von oxydations- und reduktionsreaktionen in Lösungen. Naturwissenschaften 23 (4), 64–69.
Weisz, P.B., 1967. Chapter 19-synthesis and Photosynthesis. McGraw-Hill, Inc., New York, NY.
Wert, E.C., Dong, M.M., Rosario-Ortiz, F.L., 2013. Using digital flow cytometry to assess the degradation of three cyanobacteria species after oxidation processes. Water Res. 47 (11), 3752–3761.
Wert, E.C., Korak, J.A., Trenholm, R.A., Rosario-Ortiz, F.L., 2014. Effect of oxidant exposure on the release of intracellular microcystin, MIB, and geosmin from three cyanobacteria species. Water Res. 52, 251–259.
Westerhoff, P., Rodriguez-Hernandez, M., Baker, L., Sommerfeld, M., Huang, J., Graham, N., Templeton, M.R., Zhang, Y., Collins, C., Nieuwenhuijsen, M., 2005. Seasonal occurrence and degradation of 2-methylisoborneol in water supply reservoirs. Water Res. 39 (20), 4899–4912.
Xie, P.C., Ma, J., Fang, J.Y., Guan, Y.H., Yue, S.Y., Li, X.C., Chen, L.W., 2013. Comparison of permanganate preoxidation and preozonation on algae containing water: cell integrity, characteristics, and chlorinated disinfection byproduct formation. Environ. Sci. Technol. 47 (24), 14051–14061.
Yang, Y.X., Chen, J., 2013. Advanced treatment of drinking water by ultrafiltration membrane. Adv. Mater. Res. 647, 543–547.
Zamyadi, A., Dorner, S., Sauvé, S., Ellis, D., Bolduc, A., Bastien, C., Prévost, M., 2013. Species-dependence of cyanobacteria removal efficiency by different drinking water treatment processes. Water Res. 47 (8), 2689–2700.
Zhou, S.Q., Shao, Y.S., Gao, N.Y., Deng, Y., Li, L., Deng, J., Tan, C.Q., 2014a. Characterization of algal organic matters of *Microcystis aeruginosa*: biodegradability, DBP formation and membrane fouling potential. Water Res. 52, 199–207.
Zhou, S.Q., Shao, Y.S., Gao, N.Y., Li, L., Deng, J., Zhu, M.Q., Zhu, S.M., 2014b. Effect of chlorine dioxide on cyanobacterial cell integrity, toxin degradation and disinfection by-product formation. Sci. Total Environ. 482, 208–213.